

## Modelling of AC Arcs in Three-Phase Submerged Arc Furnaces

Gudrun Saevarsdottir, Hilde Løken Larsen and Jon Arne Bakken

Norwegian University of Science and Technology, Norway

### Abstract

An improved Channel Arc Model for simulation of AC arcs on ordinary PC's is presented. In this model the arc is treated as a cylindrical current conductor with uniform radius and temperature. In order to verify the model, laboratory arcs with  $I_{rms} \approx 1000$  A, as well as industrial arcs with  $I_{rms} \approx 100$  kA, are simulated. Assuming symmetrical furnace conditions, the three-phase electric circuit is first simplified to a one-phase description which is compared to values from an industrial submerged arc furnace. In order to generalize the model, and to be able to simulate also asymmetrical furnace conditions, the complete three-phase circuit is included and results obtained from the three-phase simulations are compared with one-phase simulations. In addition, the effect of a charge current, which bypasses the arc, is shown in the three-phase description.

### Introduction

In silicon-metal and ferrosilicon furnaces, the energy needed for heating the raw materials and sustaining the chemical reactions are generated in the alternating current (AC) arcs which burn in gas-filled cavities or "craters". Due to the chemically aggressive environment and high temperatures in the metal producing part of the furnace, direct observations and measurements of the crater conditions are hardly feasible. Simulation models of the arcs can therefore improve process understanding and furnace operation.

Two models of AC arcs have been developed. In the *Magneto-Fluid-Dynamic* (MFD) model (Larsen 1995, 1996) the time dependent conservation equations of mass, momentum and energy are solved together with a conservation equation for the magnetic field. The time-dependent distributions of temperature, velocity, pressure, magnetic field and electric current density are then resolved within the arc. Due to the high level of resolution, this model demands high capacity computers and computation times in the order of hours. However, if the purpose of the model is

mainly to determine the electrical characteristic of the arc as a non-linear circuit element, the simpler *Channel Arc Model* offers a quick and easy tool. This model can be run on ordinary PCs, and is therefore suitable for on-line simulation of the furnace conditions.

### The Channel Arc Model

The Channel Arc Model presented here is an improved version of Pfeifer's (1992) model. The strength of this version is that only a limited number of parameters, which are all *physically founded*, are involved. The arc is assumed to be a cylindrical current conductor with radius  $R_k$  and a prescribed radial temperature distribution, e.g. uniform temperature  $T_k$ . An AC arc will strive towards the equilibrium state of a DC arc with current equal to the instantaneous AC current. Therefore the AC model is based on a DC model using a physically well founded time-delay factor. Basically two equations expressing the time-dependent integral energy balance and Stenbeck's energy minimum principle are solved with respect to  $R_k(t)$  and  $T_k(t)$ , taking convective and radiative heat losses into account. A detailed physical description of the Channel Arc Model is given by Larsen (1996B).

### The Electric circuit

#### The simplified symmetric case

The electric circuit of the three-phase furnace with the standard Knapsack connection is shown in Fig. 2. The electrodes form a star circuit with a floating neutral point  $O$  where the sum of the instantaneous currents is zero,  $i_1 + i_2 + i_3 = 0$ . The three-phase circuit may be simplified to the equivalent circuit presented in Fig. 1, where the current in each phase is decoupled from the currents in the two other phases. The *line* voltages,  $u_{T,12}$ ,  $u_{T,23}$ ,  $u_{T,31}$  i.e. the open-circuit voltages of the transformer secondaries, have equal rms values and a  $120^\circ$  phase delay between them.

$u_{arc,n}(t)$ ,  $n = 1, 2, 3$  is the arc voltage and  $r_n$  is the lumped loss resistance in the transformer, busbar and flexible cables in each phase. The total inductance, which includes both self-inductance and mutual inductance in each phase, is lumped into

$L'_n$ . If the circuit is assumed to be perfectly symmetric, only one phase has to be considered. We then have  $L'_1=L'_2=L'_3=L'$ ,  $r_1=r_2=r_3=r$ ,  $r_{arc,1}=r_{arc,2}=r_{arc,3}=r_{arc}$ , and the potential

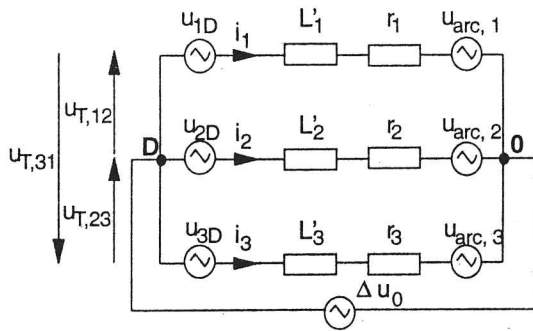


Fig. 1. The equivalent decoupled three-phase circuit diagram of a submerged-arc furnace

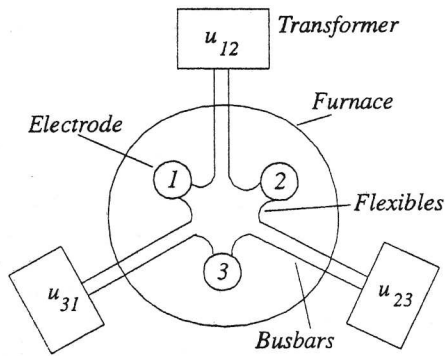


Fig. 2 The Knapsack AC connection

difference  $\Delta u_0$  in the decoupled circuit vanishes (Valderhaug 1992). The currents  $i_1$ ,  $i_2$  and  $i_3$  are then also phase delayed with  $120^\circ$  and have equal rms values. The electric circuit equation of the symmetric furnace becomes

$$\sqrt{2} U_{phase} \cos(\omega t) = L \frac{di}{dt} + ri + u_{arc} \quad (1)$$

where  $U_{phase}$  is the transformer secondary rms phase voltage. The instantaneous arc voltage  $u_{arc}$  also includes the anode and cathode falls  $U_{an}$  and  $U_{ca}$  in addition to the column voltage. The anode and cathode falls are assumed to be constant - but not necessarily equal - in each of the two half periods, and the polarity is changed when the current direction is reversed.  $\omega = 2\pi f$ , where  $f$  is the AC frequency (50 or 60 Hz).

Even in an electrically symmetrical furnace there is one property of the three-phase circuit which is not taken into account by a one-phase description. In an ideal symmetric three-phase system without zero-conductor, harmonics of

orders which can be divided by three, i.e. the 0th, 3rd, 6th, 9th... can not exist in the current waveform. These are generated by the arc and are found in the arc voltage. However, the "3n" harmonics are in phase with one another, and the harmonic current, which normally would be generated by the corresponding harmonic voltage, will therefore not find any return path. This component of the arc voltage will therefore be found at the zero-point.

### The three-phase circuit

In a furnace electrical asymmetry may occur due to asymmetric furnace design, in particular with respect to the location of the tapholes and charging shutes. Differences in the electric components in the three phases, e.g. transformers, electrode holders, phase compensation, equipment and asymmetric layout of the transformers and current conductors, are other sources of asymmetry. The three-phase circuit, now with self and mutual inductances separated, is shown in Fig. 3. Mutual inductances between the phase currents  $i_1$ ,  $i_2$ ,  $i_3$  and the line currents  $i_{12}$ ,  $i_{23}$ ,  $i_{31}$  are neglected, but can easily be included in the circuit.

Using Kirchoff's current law and summing up the voltage drops of the current loops 1201, 2302 and 3103, six equations are obtained.

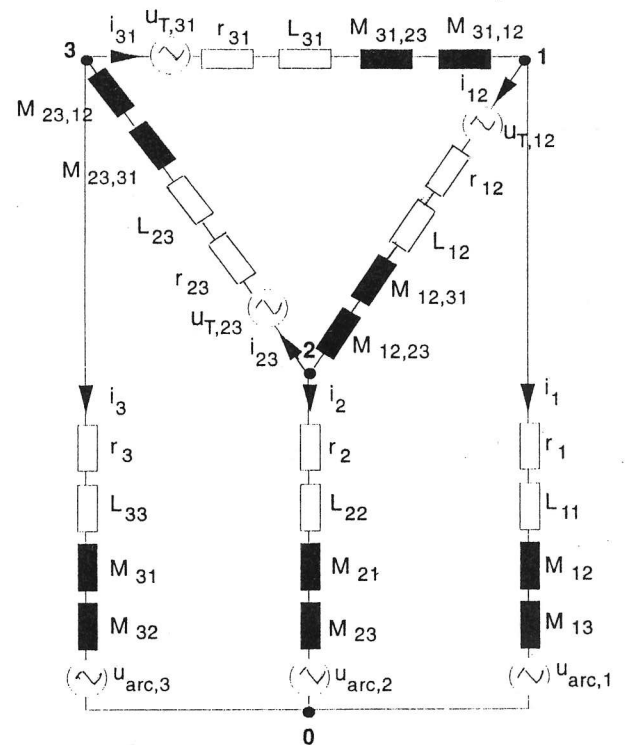


Fig. 3 Three-phase circuit diagram

The currents of the circuit are found by first solving the set of the three coupled equations, which can be arranged in the matrix form:

$$\begin{bmatrix} -L_{12}-L_1-L_2 & L_2-M_{12,23} & L_1-M_{12,31} \\ L_2-M_{23,12} & -L_{23}-L_2-L_3 & L_3-M_{23,31} \\ L_1-M_{31,12} & L_3-M_{31,23} & -L_{31}-L_3-L_1 \end{bmatrix} \begin{bmatrix} \frac{di_{12}}{dt} \\ \frac{di_{23}}{dt} \\ \frac{di_{31}}{dt} \end{bmatrix} =$$

$$\begin{bmatrix} u_{T,12}-u_{arc,1}+u_{arc,2}+(r_{12}+r_1+r_2)i_{12}-r_1i_{31}-r_2i_{23} \\ u_{T,23}-u_{arc,2}+u_{arc,3}+(r_{23}+r_2+r_3)i_{23}-r_2i_{12}-r_3i_{31} \\ u_{T,31}+u_{arc,1}-u_{arc,3}+(r_{31}+r_3+r_1)i_{31}-r_3i_{23}-r_1i_{12} \end{bmatrix} \quad (2)$$

where the phase inductances  $L_i$  include the mutual inductances  $M_{ij}$ :

$$\begin{aligned} L_1 &= L_{11} - M_{12} - M_{31} + M_{23} \\ L_2 &= L_{22} - M_{23} - M_{12} + M_{31} \\ L_3 &= L_{33} - M_{31} - M_{23} + M_{12} \end{aligned} \quad (3)$$

When the line currents  $i_{12}$ ,  $i_{23}$  and  $i_{31}$  have been determined, the phase currents  $i_1$ ,  $i_2$  and  $i_3$  are calculated from Kirchoff's current law:

$$\begin{aligned} i_1 &= i_{31} - i_{12} \\ i_2 &= i_{12} - i_{23} \\ i_3 &= i_{23} - i_{31} \end{aligned} \quad (4)$$

### Solution procedure

The solution procedure of the AC Channel Arc Model is as following: The arc length  $H$  and a starting value for the current  $I_{start}$  is given. The current is later calculated as a function of time by a simple explicit integration of the circuit equation (1) in the "one-phase" model or integration of (2) in combination with (3) and (4) in the complete model. Flow schemes for the Channel Arc Model are described by Larsen (1996 B)

## Modelling Results

### Laboratory arcs

There are many uncertainties connected with measurements of industrial high current arcs ( $I_{rms} \sim 100$  kA). The voltage measurements can be subject to various random as well as systematic errors and may be difficult to interpret, e.g. to ascertain where in the electric circuit the voltage is measured. Furthermore, exact information about the gas composition and the arc length are difficult to obtain. It was therefore considered an important task first to verify the model by comparison with measurements on relatively low current arcs ( $I_{rms} \sim 1000$  A) carried out under controlled laboratory conditions. The experiment and comparison with simulation is described in detail by Larsen(1996B) Measurements of current and arc voltage were made for different nominal arc lengths and transformer settings. The arc burned between two graphite electrodes in an argon atmosphere of 1 bar pressure.

Measurements of current and arc voltage were made for different nominal arc lengths and transformer settings. The arc burned between two graphite electrodes in an argon atmosphere of 1 bar pressure. In advance of the experiments, the arc was replaced by known resistances, and the resistance  $r$  and inductance  $L$  of the one-phase circuit were found. Different impedance values were realized by adjusting the reactance of the welding transformers used as voltage source.

As the simulation results depend on the choice of model parameters, the important aspect is not whether the calculated current and voltage agree exactly with the measured ones, but whether the current and voltage waveforms and the rms current-voltage characteristics for different arc lengths and transformer settings show the correct trends. As an example, calculated dynamic current-voltage characteristics for a 4 cm long argon arc will be presented and compared with the corresponding measured waveforms. Fig. 3 shows the calculated (thick lines) and measured (thin lines) current and voltage waveforms for the 4 cm argon arc. The waveforms are in good agreement with the measured ones with an almost sinusoidal current and a more square shaped voltage.

The calculated and measured rms currents and voltages together with the DC components of the current and voltage are shown in Table 2.

Table 2. Measured and calculated results for the 4 cm argon arc.

Lab. Ar arc	$I_{rms}$ (A)	$U_{rms}$ (V)	$I_{dc}$ (A)	$U_{dc}$ (V)
Meas.	651±8	44±1	87.8	0.4
Calc.	687	38.0	2.8	0.09

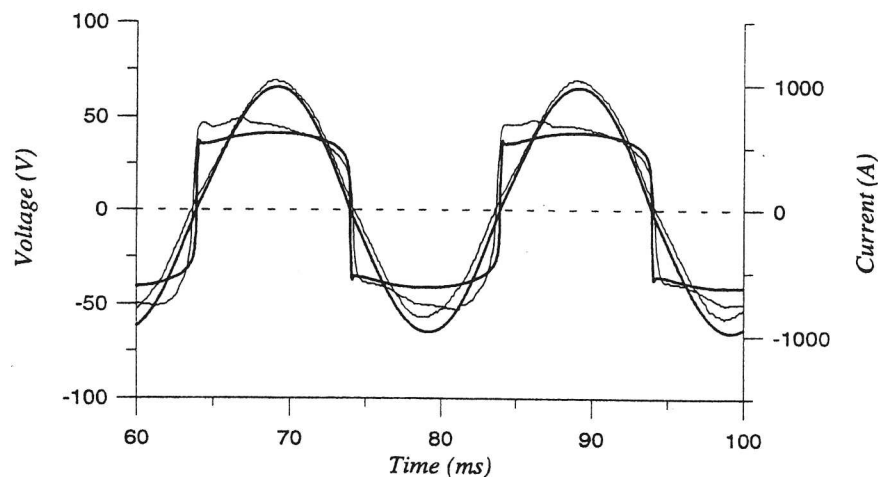


Fig. 3. Calculated (thick lines) and measured (thin lines) currents (almost sinusoidal) and voltages (almost square shaped) versus time for the 4 cm argon arc

Compared with the measured values, the calculated voltage is lower than the measured one, and the calculated current higher. However, the sensitivity analysis of the model parameters showed that especially the voltage level depends on the parameter values chosen. The measured current contains a significant DC component of 88 A, and the voltage a much smaller DC component of 0.4 V. The calculated current and voltage DC components are negligible and the small values found must be due to numerical inaccuracies. As long as the same parameters are used in both half periods, there is no reason why the structure-less Channel Arc Model should give rise to DC components or even harmonics. The even harmonics in the calculated signals are negligible. Asymmetry can, however, be introduced in the Channel Arc Model by applying different anode and cathode fall voltages, anode work functions or cathode current densities in the two half periods.

## Industrial Arcs

### Symmetrical case

Comparisons have been made between the three-phase (3P) and one-phase (1P) descriptions, using identical model parameters and data for argon rather than SiO-CO. Fig. 4 shows the waveforms of the arc current and voltage for the 1P and 3P simulations. The current waveform obtained by the 3P

simulation differs from the 1P simulation in that the current increases much faster after passing through zero, resulting in an absence of the current-free period obtained in the 1P simulation. The amplitude of the 3P arc current is somewhat lower than that of the 1P current, but the RMS currents for the two cases are equal. Another difference is that the three phases clearly affect one another in such a way that the gradient of the  $i_1$  curve has a discontinuity where the currents in the other phases,  $i_2$  and  $i_3$ , pass zero.

Fig. 5 shows the Fourier analysis of the arc currents and voltages. The main difference between the 1P and 3P current curves, is that the  $3n$  harmonics are missing in the 3P case. This is consistent with Kirchoff's current law at the star point. The difference in the voltage waveforms in the two cases is not as great, as that of the currents.

### Asymmetrical case

A simulation for an asymmetrical case is also presented. Two of the arcs have the same length, 10 cm, but the third one is 30 cm long. All other parameters were the same as in the symmetrical case. Fig. 6 shows the current waveforms for this case, and the Fourier spectrum of the three phases. Here the  $3n$  Fourier components appear in all the three phases. It can be seen that phase 3, with the 30 cm arc, carries a much smaller current than phases 1 and 2, and that the maxima and minima of phases 1 and 2 are shifted such that one phase has maximum while the other has minimum,

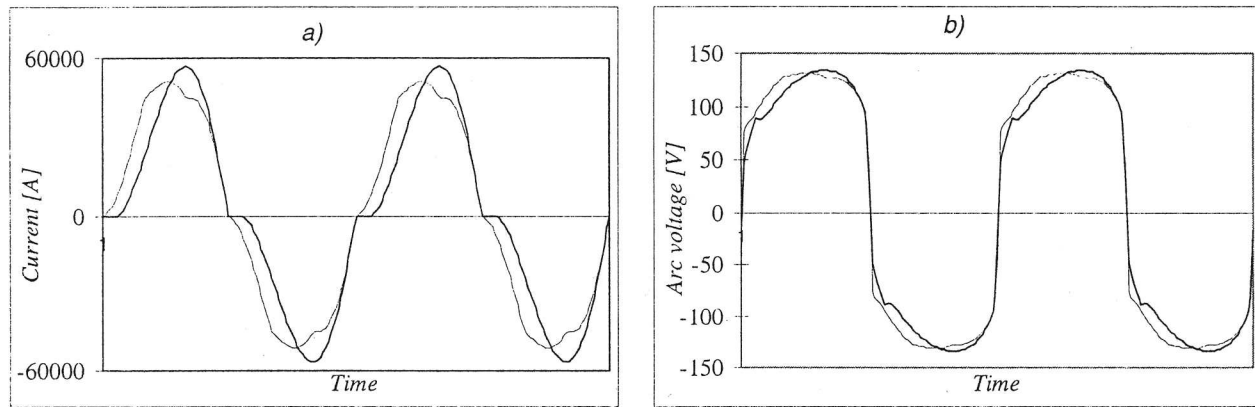


Fig. 4. Simulated arc a) current and b) voltage waveforms obtained by the one-phase (thick line) and the three-phase model (thin line) respectively.

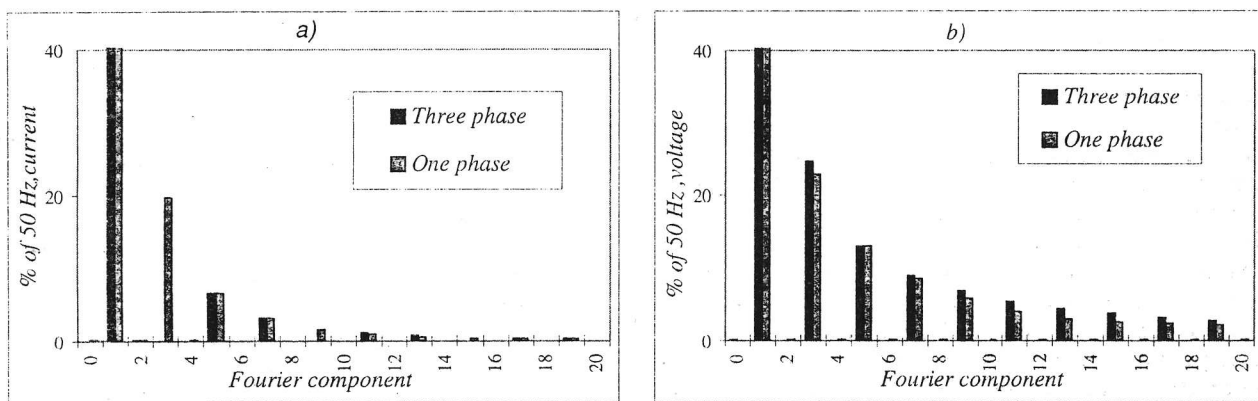


Fig. 5. Fourier components for a) current and b) voltage for the 10 cm long argon arc. in the one-phase and symmetrical three-phase cases, respectively

and vice versa. Thus the three phases have great effect on one another, and extreme conditions in one of the phases alter the characteristics of the two other phases to a large extent.

### The effect of charge current

In a submerged arc furnace, a part of the current flows from the electrode to the melt, through the charge, without passing through the electric arc. This has been believed to change the characteristics of the system significantly. Therefore the circuit was modified by placing a resistance in parallel with the arc. Fig. 7 shows the electrode current and voltage along with the charge and arc currents for the simulation presented here. In this simulation the charge current amounts to about 20% of the total electrode phase current. Also a Fourier analysis of the electrode phase current is compared with a simulation with all parameters identical apart from the absence of charge current. One of the main features is an increased electrode current, which is to be expected as the

phase resistance is decreased by the presence of the charge resistance. Another important factor is that the fractional content of higher harmonics in the phase current is decreased when the charge current is taken into consideration, that is the current waveform is more sinusoidal.

### Conclusions

An improved version of the Channel Arc Model in combination with a complete three-phase electric circuit description has been presented. For laboratory arcs (~1000 A) in argon satisfactory agreement between simulated and measured current and voltage waveforms are obtained. Improved sub-models for the cathode and anode regions are being developed presently.

The model has been generalized by including all three phases in the electric circuit, allowing for electrical asymmetry and interaction between the phases. The DC component and the 3rd, 6th, 9th, etc. harmonics of the

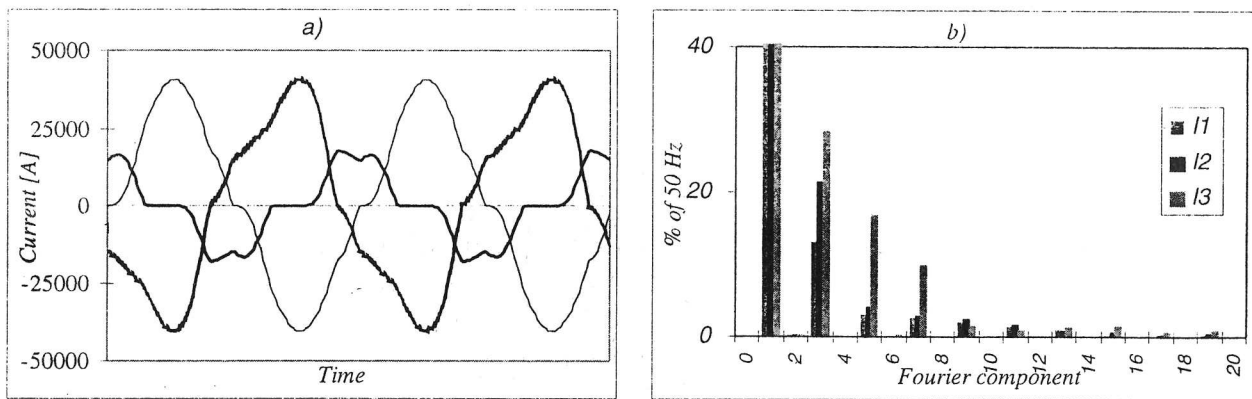


Fig. 6. Simulated arc currents obtained from an asymmetrical three-phase simulation, a) shows the current waveforms, and b) its Fourier spectrum.

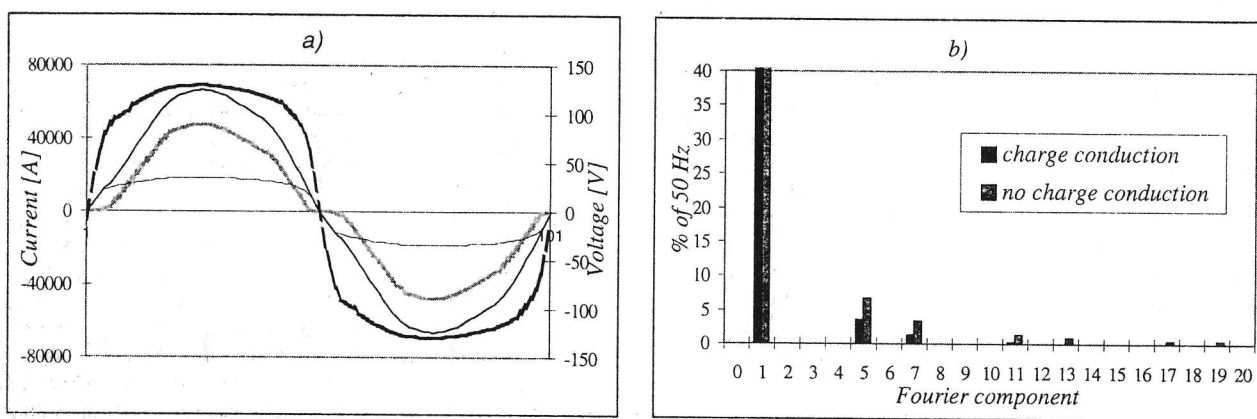


Fig. 7. Simulated arc currents and voltages from a symmetrical three-phase simulation taking charge current into account. a) shows the waveforms of the phase current (black line), charge current (thin line), arc current (thick grey line) and arc voltage (Thick black line). b) shows the Fourier components for the phase current compared with those of a simulation without charge conduction.

current disappear in a symmetric furnace. In a one-phase description, however, these components will appear. Taking charge conduction into account in the simulation, gives a more sinusoidal waveform for the phase current. The improved Channel Arc Model in combination with the general three-phase circuit equations has potential applications in the operation of Submerged Arc Furnaces for silicon metal and ferrosilicon production as well as Electric Arc Furnaces for steelmaking.

**References**

Larsen HL, Bakken JA. A Numerical Model For the AC-Arc in the Silicon Metal Furnace, In Proceedings, IFACON-7 1995 , Trondheim, Norway.

Larsen HL. AC electric arc models for a laboratory set-up and a silicon metal furnace, Dr. Ing. thesis, Norwegian University of Science and Technology, Trondheim 1996.

Larsen HL, Saevarsdottir G , Bakken JA. In Proceedings, EFC-53 1996(B) , Dallas, Tx, U.S.A.

Pfeifer H. Energietechnische Untersuchung der Plasmatechnik bei der Stahlerzeugung, Habilitationsschrift vom Fachbereich Maschinentechnik der Universität Gesamthochschule Siegen, Verlag Stahleisen GmbH, Düsseldorf, 1992

**Aknowledgements**

This research has been financially supported by the Norwegian Ferroalloy Producers Research Association (FFF) and The Research Council of Norway (NFR). They are both greatly acknowledged